Supplementary Materials:

Robert M. Healy [1,*], Uwayemi M. Sofowote [1], Jonathan M. Wang [1], Qingfeng Chen[1] and Aaron Todd [1]

[1] Environmental Monitoring and Reporting Branch, Ontario Ministry of the Environment Conservation and Parks, Toronto, ON M9P 3V6, Canada
* Correspondence: robert.healy@ontario.ca.

MECP mobile monitoring platform:

Figure S1. MECP mobile monitoring platform interior and exterior.

PMF Analysis and Optimization:

Factor solutions (FS) featuring four to eight factors were obtained from the base PMF analyses. Table S1, S2 and S3 show the input data summary statistics, the fits from the base results and the scaled residuals beyond 3 standard deviations, respectively. The results indicated that the seven-factor solution (7FS) and the eight-factor solution (8FS) were similar in terms of their performance metrics: Q, scaled residuals (range: 3-4) and Q/Q_{exp}. Figure S2 shows a plot of the reduction in Q with each successive factor obtained. The percent decrease in Q moving from a 7FS to an 8FS compared to previous decreases was not considered to be large enough to justify using an 8FS. Furthermore, the 8FS extracted a *m/z* 105-dominated factor (styrene), but the modelling fit was poor and therefore this extra factor was not considered to be physically meaningful. Thus, the 7FS was deemed to be optimal. Q/Q_{exp} for the factor profiles and the summed contributions for the base 7FS were <0.6 and <2.5, respectively, as shown in Figure S3.

Table S1. PMF input statistics for the retained zero-background subtracted ions (ncps units).

Species	Category	S/N	Min	25th	Median	75th	Max	% Modeled Samples	% Raw Samples
m31_0	Weak	0.205	-13.079	13.296	18.566	23.841	158.543	99.56 %	100.00 %
m33_0	Strong	4.427	88.968	191.515	221.180	280.723	2573.377	99.56 %	100.00 %
m40_0	Strong	3.466	3.936	40.821	68.528	94.208	258.622	99.56 %	100.00 %
m41_0	Strong	3.010	5.199	44.688	58.936	86.746	1132.921	99.56 %	100.00 %
m42_0	Weak	2.518	2.101	25.091	33.950	62.571	782.718	99.56 %	100.00 %
m43_0	Strong	1.683	-13.400	21.622	38.096	66.931	559.454	99.56 %	100.00 %
m44_0	Weak	0.183	-2.783	6.649	9.944	14.314	45.453	99.56 %	100.00 %
m45_0	Strong	0.277	-40.258	-15.691	-1.573	13.166	288.960	99.56 %	100.00 %
m46_0	Weak	0.227	-14.535	2.083	10.190	16.724	98.778	99.56 %	100.00 %
m48_0	Weak	0.067	-3.769	3.443	5.628	8.424	24.402	99.56 %	100.00 %
m50_0	Weak	0.004	-12.874	-0.996	2.166	5.571	42.919	99.56 %	100.00 %
m51_0	Strong	0.266	-1.810	4.749	7.598	11.811	102.604	99.56 %	100.00 %
m53_0	Weak	0.074	-3.593	3.230	4.866	6.869	136.297	99.56 %	100.00 %
m54_0	Weak	0.041	-4.081	2.143	3.773	5.681	126.059	99.56 %	100.00 %
m57_0	Strong	3.673	8.139	42.115	53.755	77.690	2935.156	99.56 %	100.00 %
m58_0	Weak	0.184	-2.442	4.798	6.902	9.494	160.081	99.56 %	100.00 %
m59_0	Strong	9.185	73.992	173.803	195.943	221.692	2153.201	99.56 %	100.00 %
m60_0	Weak	0.064	-6.720	2.989	5.421	8.109	88.890	99.56 %	100.00 %
m63_0	Weak	0.097	0.059	5.436	6.915	8.698	19.183	99.56 %	100.00 %
m69_0	Strong	0.567	1.044	9.393	12.320	17.411	150.810	99.56 %	100.00 %
m70_0	Weak	0.051	-1.616	3.334	4.751	6.460	38.910	99.56 %	100.00 %
m71_0	Strong	0.499	-4.666	5.663	10.202	15.669	164.510	99.56 %	100.00 %
m73_0	Strong	1.007	-3.728	7.344	12.206	22.049	2785.223	99.56 %	100.00 %
m74_0	Weak	0.069	-4.129	0.890	2.347	4.102	149.662	99.56 %	100.00 %
m75_0	Weak	0.168	-8.463	0.383	3.187	9.210	266.126	99.56 %	100.00 %
m77_0	Strong	0.979	-3.318	6.120	11.089	17.710	153.907	99.56 %	100.00 %
m78_0	Strong	1.083	-2.359	2.855	4.732	15.490	343.674	99.56 %	100.00 %
m79_0	Strong	4.715	0.094	13.528	36.628	327.927	6906.583	99.56 %	100.00 %
m80_0	Strong	1.574	-1.422	3.706	5.978	25.339	488.900	99.56 %	100.00 %
m81_0	Weak	0.175	-1.595	4.385	6.250	8.803	48.502	99.56 %	100.00 %
m83_0	Weak	0.137	-1.205	4.094	5.903	8.361	95.377	99.56 %	100.00 %
m85_0	Weak	0.092	-1.785	3.009	4.662	6.902	106.536	99.56 %	100.00 %
m87_0	Weak	0.184	-0.709	4.500	6.684	9.725	23.345	99.56 %	100.00 %
m89_0	Weak	0.038	-4.224	0.120	1.598	3.495	145.068	99.56 %	100.00 %
m93_0	Strong	1.346	-1.759	6.279	10.424	19.889	763.808	99.56 %	100.00 %
m94_0	Weak	0.059	-4.640	0.114	1.504	3.445	67.152	99.56 %	100.00 %
m96_0	Weak	0.141	-1.630	4.819	6.666	8.269	17.699	99.56 %	100.00 %
m97_0	Weak	0.238	1.640	6.921	8.739	10.894	98.792	99.56 %	100.00 %
m98_0	Weak	0.118	-0.338	4.511	5.929	7.240	14.699	99.56 %	100.00 %
m99_0	Weak	0.046	-2.949	2.113	3.626	5.662	43.299	99.56 %	100.00 %
m101_0	Strong	0.286	0.346	5.198	7.156	10.061	214.831	99.56 %	100.00 %
m105_0	Weak	0.429	-3.809	1.260	3.241	6.403	628.896	99.56 %	100.00 %
m106_0	Weak	0.018	-9.243	-1.497	-0.187	1.234	58.564	99.56 %	100.00 %
m107_0	Weak	1.954	4.505	11.666	14.794	23.036	999.739	99.56 %	100.00 %
m108_0	Weak	0.068	-3.954	0.651	1.726	3.008	95.198	99.56 %	100.00 %
m109_0	Weak	0.040	-7.780	0.884	3.482	7.004	28.034	99.56 %	100.00 %
m111_0	Weak	0.009	-5.130	-0.848	0.279	1.744	55.377	99.56 %	100.00 %
m115_0	Weak	0.085	-4.032	0.407	2.265	5.118	69.094	99.56 %	100.00 %
m117_0	Weak	0.143	0.479	4.066	5.350	6.923	20.689	99.56 %	100.00 %
m121_0	Weak	0.366	-1.194	3.210	4.828	7.695	194.790	99.56 %	100.00 %
m122_0	Weak	0.036	-2.302	1.389	2.431	3.834	20.926	99.56 %	100.00 %
m124_0	Strong	0.337	-4.510	5.194	8.461	13.614	31.971	99.56 %	100.00 %
m125_0	Weak	0.007	-3.383	0.250	1.249	2.503	26.642	99.56 %	100.00 %
m133_0	Weak	0.007	-2.592	0.181	0.974	1.937	21.524	99.56 %	100.00 %
m135_0	Weak	0.100	-2.712	1.165	2.193	3.756	79.873	99.56 %	100.00 %

m137_0	Weak	0.007	-5.012	-0.535	0.478	1.681	16.349	99.56 %	100.00 %
m139_0	Weak	0.002	-3.872	-1.016	-0.006	1.159	17.392	99.56 %	100.00 %
m143_0	Weak	0.057	-2.101	2.269	3.828	5.747	21.280	99.56 %	100.00 %
m147_0	Weak	0.006	-3.277	-0.226	0.528	1.421	39.453	99.56 %	100.00 %
m149_0	Weak	0.019	-2.233	0.777	1.627	2.673	69.704	99.56 %	100.00 %
m153_0	Weak	0.000	-3.295	-0.841	-0.061	0.854	8.001	99.56 %	100.00 %
m161_0	Weak	0.168	-2.435	2.263	4.078	6.818	61.825	99.56 %	100.00 %

Table S2. Model fits for all ions used in the PMF analyses.

Species	Intercept	Slope	SE	r^2	KS Test Stat	KS Test P Value
m31_0	4.81	0.73	5.53	0.67	0.03	5.31E-09
m33_0	67.74	0.71	49.79	0.77	0.10	0
m40_0	2.27	0.97	7.28	0.98	0.01	0.181874
m41_0	6.99	0.89	11.01	0.95	0.08	0
m42_0	27.81	0.32	19.79	0.28	0.17	0
m43_0	6.20	0.85	15.68	0.84	0.04	2.01E-12
m44_0	1.55	0.86	2.41	0.86	0.01	0.31
m45_0	8.59	0.65	7.99	0.87	0.05	0
m46_0	5.88	0.32	6.10	0.28	0.08	0
m48_0	1.56	0.73	1.84	0.71	0.02	0.02
m50_0	2.02	0.33	2.14	0.39	0.02	5.06E-04
m51_0	1.85	0.78	2.22	0.83	0.02	2.69E-03
m53_0	2.30	0.56	2.17	0.66	0.08	0
m54_0	1.89	0.54	1.93	0.64	0.06	0
m57_0	11.15	0.85	19.20	0.97	0.17	0
m58_0	0.91	0.88	1.92	0.92	0.02	0.03
m59_0	28.38	0.85	22.43	0.92	0.09	0
m60_0	2.22	0.64	1.93	0.73	0.03	1.05E-07
m63_0	2.45	0.64	1.53	0.54	0.01	0.39
m69_0	5.62	0.57	3.11	0.64	0.05	0
m70_0	1.61	0.66	1.21	0.64	0.01	0.52
m71_0	2.86	0.72	3.62	0.75	0.03	1.49E-07
m73_0	2.15	0.90	6.95	0.99	0.06	0
m74_0	0.28	0.91	1.45	0.94	0.01	0.55
m75_0	1.41	0.74	3.67	0.83	0.05	0
m77_0	3.98	0.63	5.15	0.70	0.06	0
m78_0	0.22	0.97	2.68	0.99	0.09	0
m79_0	-1.98	1.01	21.49	1.00	0.19	0
m80_0	-0.29	1.01	2.16	1.00	0.03	4.22E-05
m81_0	1.68	0.74	1.88	0.73	0.04	9.04E-11
m83_0	2.31	0.63	1.99	0.67	0.05	0
m85_0	1.94	0.61	1.75	0.64	0.05	1.11E-16
m87_0	1.69	0.75	1.69	0.73	0.02	0.01
m89_0	0.92	0.57	2.08	0.59	0.06	0
m93_0	0.38	0.97	7.03	0.97	0.17	0
m94_0	0.64	0.82	1.42	0.87	0.01	0.12
m96_0	3.53	0.45	1.22	0.46	0.01	0.28
m97_0	3.34	0.62	1.94	0.57	0.03	1.54E-07
m98_0	2.93	0.49	1.07	0.45	0.01	0.78
m99_0	1.25	0.68	1.32	0.70	0.01	0.10
m101_0	0.89	0.87	1.96	0.93	0.01	0.53
m105_0	4.60	0.03	4.67	0.03	0.23	0
m106_0	0.45	0.10	0.95	0.12	0.11	0
m107_0	16.44	0.18	20.43	0.18	0.23	0
m108_0	1.72	0.19	2.01	0.19	0.16	0

m109_0	1.43	0.68	1.94	0.71	0.01	0.13
m111_0	0.84	0.36	0.77	0.56	0.04	2.17E-11
m115_0	0.70	0.77	2.43	0.74	0.04	4.74E-10
m117_0	1.81	0.65	1.27	0.53	0.01	0.77
m121_0	1.95	0.68	4.05	0.75	0.12	0
m122_0	0.77	0.71	0.97	0.72	0.01	0.14
m124_0	1.21	0.87	2.04	0.88	0.02	3.07E-04
m125_0	0.68	0.53	0.88	0.57	0.02	0.04
m133_0	0.60	0.46	0.73	0.49	0.02	9.53E-05
m135_0	1.52	0.42	1.80	0.49	0.11	0
m137_0	0.69	0.28	0.67	0.39	0.05	4.44E-16
m139_0	0.63	0.29	0.41	0.58	0.02	1.17E-04
m143_0	1.81	0.52	1.35	0.49	0.02	2.42E-03
m147_0	0.57	0.28	0.60	0.36	0.04	5.71E-14
m149_0	1.20	0.29	0.92	0.30	0.05	0
m153_0	0.42	0.22	0.29	0.48	0.02	0.01
m161_0	0.99	0.74	2.01	0.70	0.04	6.66E-15

Table S3. Scaled residuals beyond 3 standard deviations (dates by species).

Species	Date_Time	Residuals
m33_0	18/06/2020	3.16
m33_0	24/06/2020	3.253
m105_0	16/06/2020	3.078
m105_0	16/06/2020	3.058
m107_0	16/06/2020	3.185
m107_0	16/06/2020	3.112
m107_0	16/06/2020	3.221
m107_0	16/06/2020	3.122
m107_0	16/06/2020	3.304
m107_0	16/06/2020	3.316
m107_0	16/06/2020	3.197
m107_0	16/06/2020	3.188
m107_0	16/06/2020	3.037
m107_0	16/06/2020	3.058
m107_0	16/06/2020	3.038
m107_0	16/06/2020	3.291
m107_0	16/06/2020	3.046
m107_0	16/06/2020	3.092
m107_0	16/06/2020	3.177

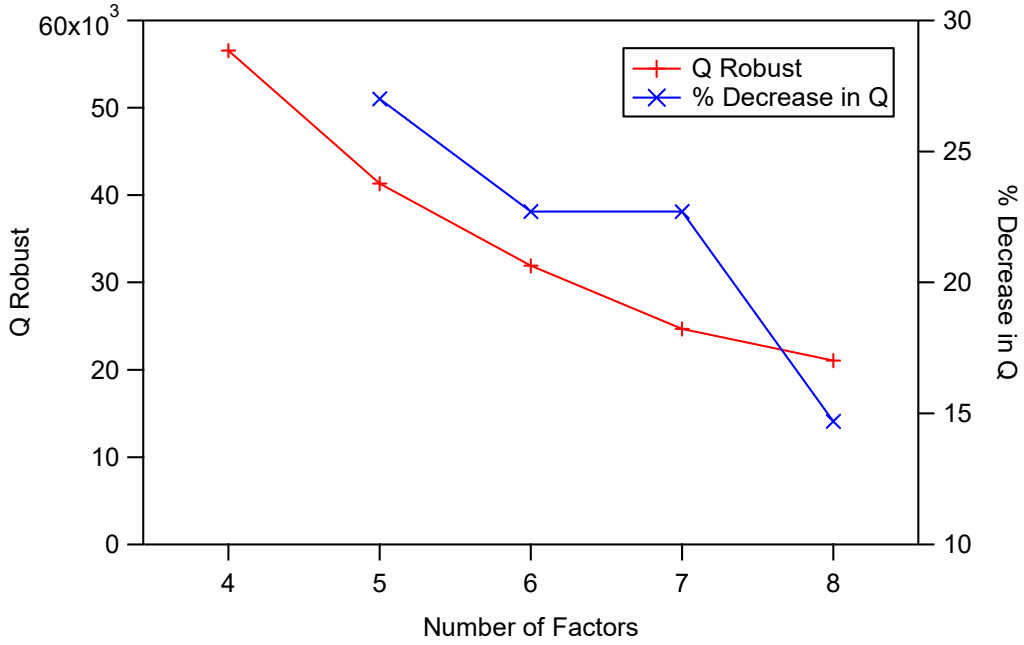

Figure S2. Reduction in Q with increasing factor number.

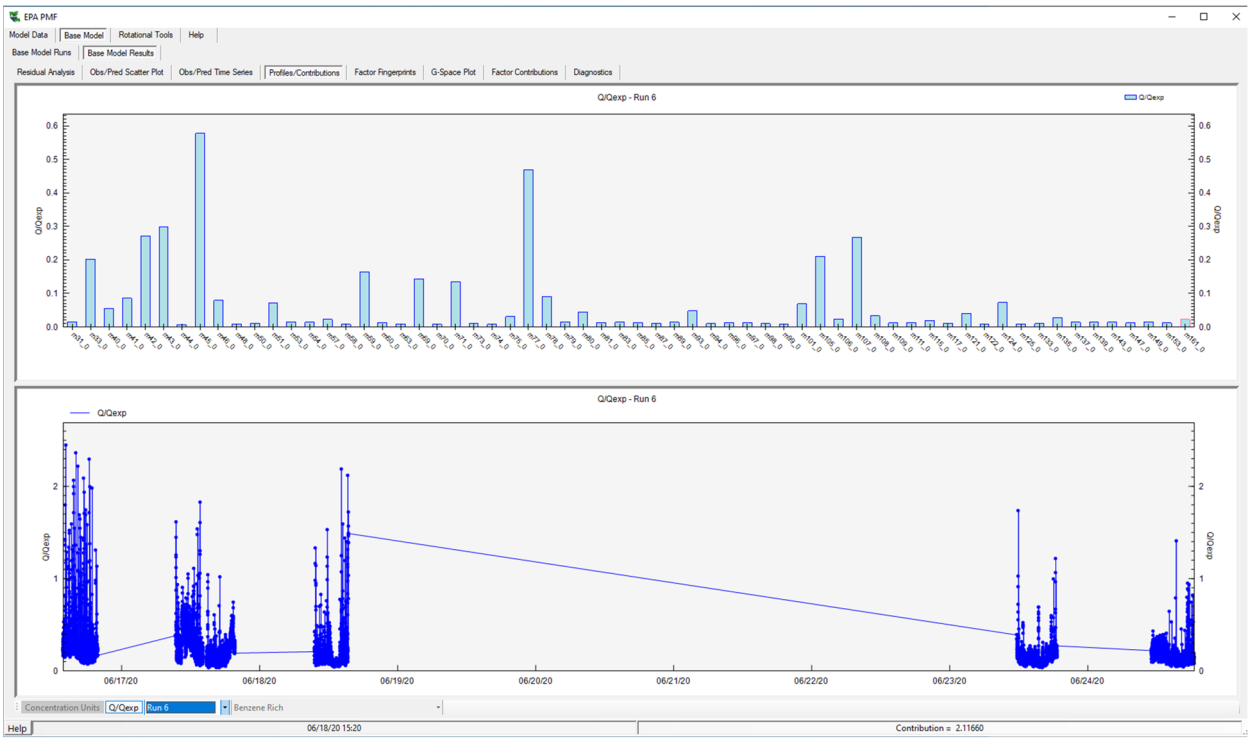

Figure S3. Q/Q_{exp} for the factor profiles (top) and their summed contributions to total ion counts (bottom) for the base seven-factor solution.

Further runs were initiated to assess the extent to which the base factor solutions were affected by random errors and rotational ambiguity both singly and jointly [1]. 100 bootstrap (BS) runs were initiated to assess the random errors. The results were satisfactory, i.e., all factors had at least 80% of their bootstrapped factors mapped to their base factors (Table S4). These bootstrap runs were then followed by a displacement run (DISP) and a hybrid BS-DISP to assess the extent of rotational ambiguity both singly and coupled

with random errors, respectively. While the DISP run was devoid of factor swaps at all dQ_{max} levels, there were some swaps in the BS-DISP runs, the remedy for which was the application of constraints to the factor solution.

Table S4. Error estimation summary (BS, DISP, BS-DISP) for the base model. Note that factor swaps were present in the BS-DISP results.

Time of run:	03/01/21 13:14							
Concentration file:	C:\Users\...\Rob's VOC_PTR_MS_Data_2020\AVG_sarnia_15s_Yemi_Trim_III.xlsx							
Uncertainty file:	C:\Users\...\Rob's VOC_PTR_MS_Data_2020\ERR_sarnia_15s_Yemi_Trim_III.xlsx							
Configuration file:	C:\Users\...\Rob's VOC_PTR_MS_Data_2020\7_FS\7FS_SARNIA.cfg							
BS-DISP Displaced Species:								
m33_0								
m40_0								
m57_0								
m59_0								
m79_0								
DISP Displaced Species:								
m33_0								
m40_0								
m41_0								
m43_0								
m45_0								
m51_0								
m57_0								
m59_0								
m69_0								
m71_0								
m73_0								
m77_0								
m78_0								
m79_0								
m80_0								
m93_0								
m101_0								
m124_0								
BS-DISP Diagnostics:								
# of Cases Accepted:	81							
% of Cases Accepted:	81%							
Largest Decrease in Q:	-44.87400055							
%dQ:	-0.216708281							
# of Decreases in Q:	1							
# of Swaps in Best Fit:	16							
# of Swaps in DISP:	2							
Swaps by Factor:	3	1	13	12	8	0	1	3
DISP Diagnostics:								
Error Code:	0							
Largest Decrease in Q:	-0.165000007							
%dQ:	-0.000796828							
Swaps by Factor:	0	0	0	0	0	0	0	0
BS Mapping:								
	Factor 1	Factor 2	Factor 3	Factor 4	Factor 5	Factor 6	Factor 7	Unmapped

Boot Factor 1	100	0	0	0	0	0	0	0
Boot Factor 2	0	100	0	0	0	0	0	0
Boot Factor 3	0	6	88	1	0	3	0	2
Boot Factor 4	0	6	0	93	0	1	0	0
Boot Factor 5	0	15	0	0	82	2	0	1
Boot Factor 6	0	0	0	0	0	100	0	0
Boot Factor 7	0	2	0	1	0	0	97	0

Three constraints were developed and applied to the solution. As mentioned above, *m*/*z* 105 had appeared as a distinct factor in the 8FS and was also characterized by an unexpectedly low contribution for the Petroleum factor in the base 7FS. A step-wise approach of constraining this variable was applied as discussed in Sofowote et al., (2015) [2], i.e., hard and unwanted rotations with their associated high increase in dQ values were examined for, followed by BS, DISP and BS-DISP, then subsequent adjustments to the number of constraints applied in that sequence. The initial explained variances (EV) of the *m*/*z* 105 variable in the base 7FS were as follows: Background/Acetone Factor EV ~45%, Chemical Waste Factor EV ~20%, Petroleum Factor EV ~20% (unexpectedly low relative to the other aromatics). Thus, constraints were applied to pull *m*/*z* 105 down maximally in both the Background/Acetone and Chemical Waste Factors, while pulling it up maximally in the Petroleum Factor (each with a maximum allowed %dQ absolute change of 0.5%). Applying these three constraints together resulted in swaps during the BS-DISP phase, indicating that new, unwanted rotations had occurred. The factor swaps persisted when the number of constraints was reduced from three to two. Not until only the most critical constraint (pulling up *m*/*z* 105 in the Petroleum Factor) was singly applied did the factor swaps cease in the BS-DISP phase (Figure S4), with Petroleum then explaining a more realistic ~45% of the *m*/*z* 105 variance in the constrained solution. Thus, the final constrained 7FS was used for source apportionment purposes. Q/Q_{exp} for the factor profiles and the summed contributions for the final constrained 7FS were <0.4 and <0.5, respectively, as shown in Figure S5. The overall apportionment results for the base and final constrained 7FS are shown in Figures S6-S8. A scatter plot of the modelling fit performance for the final constrained 7FS as assessed by the correlation of the modelled and observed sum of PTR-ToF-MS ion counts is shown in Figure S9.

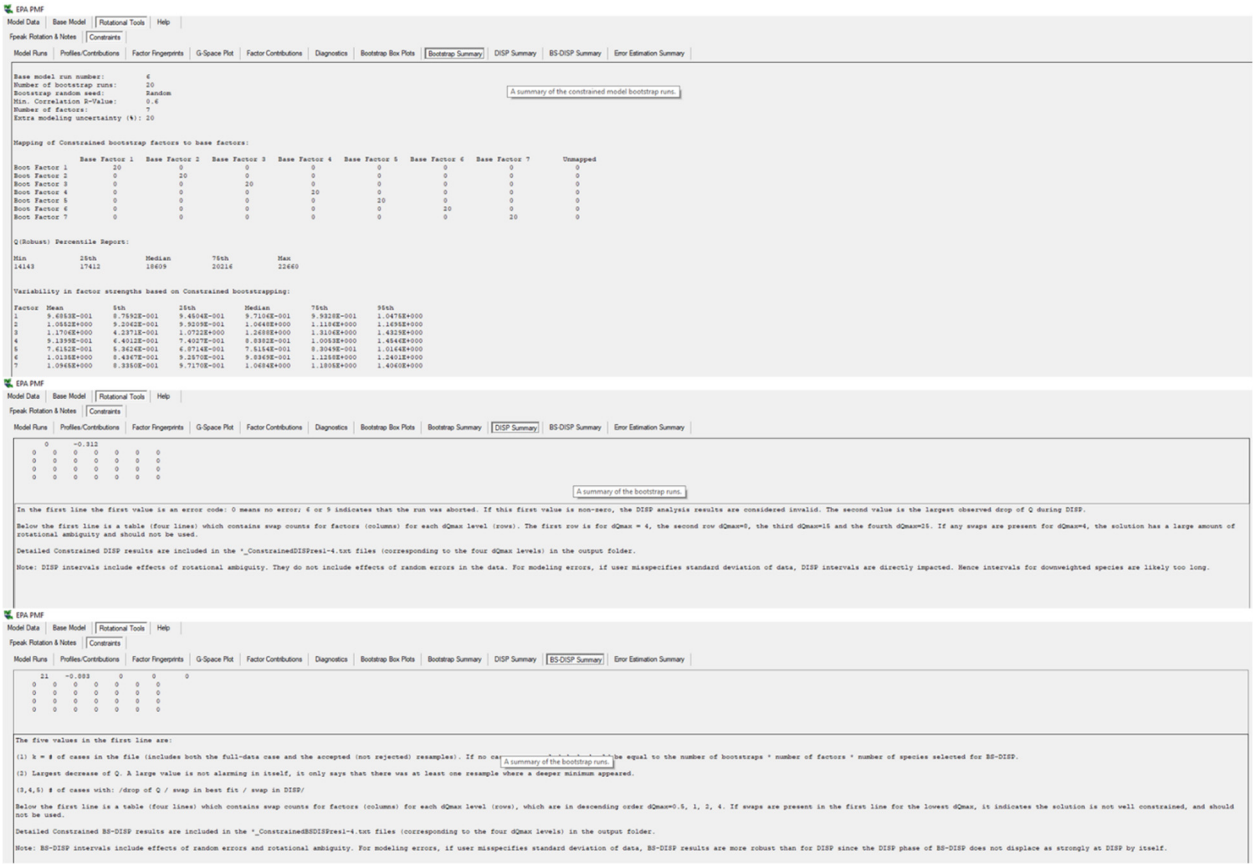

Figure S4. Stacked screenshots of the final constrained 7FS run showing no factor swaps in DISP and BS-DISP runs after the application of the final single constraint. .

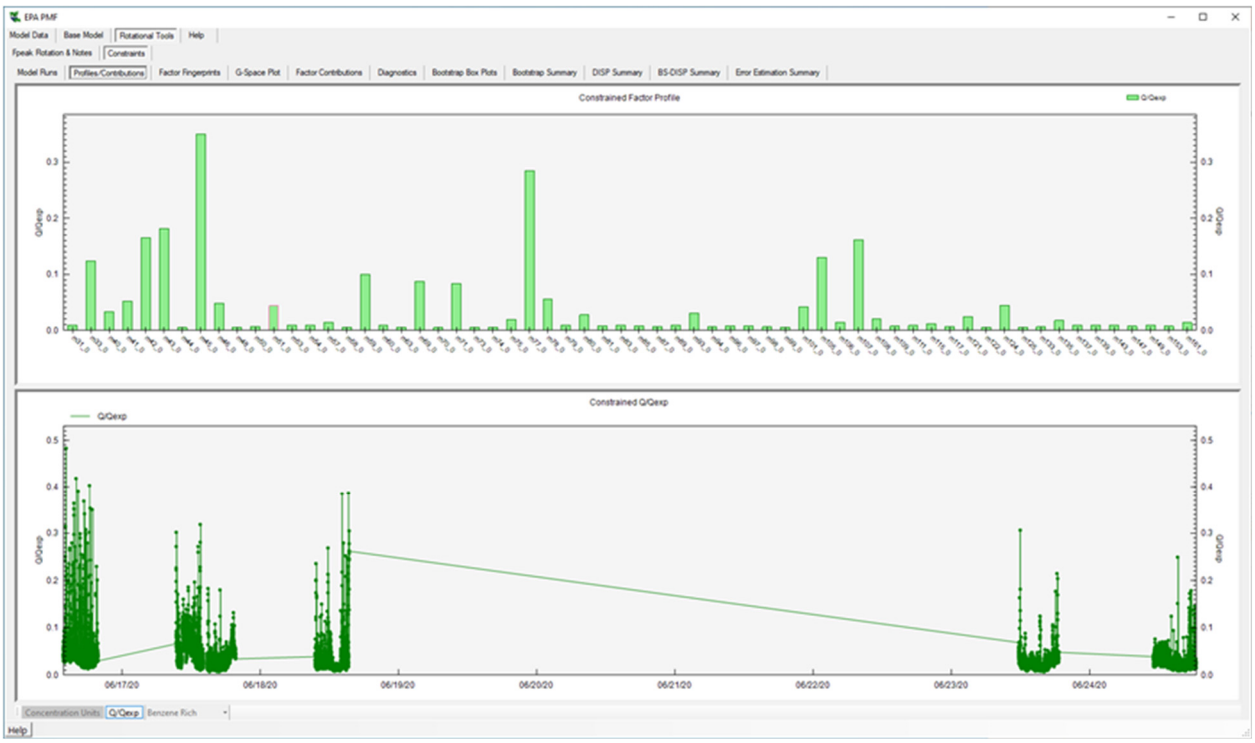

Figure S5. Q/Q_{exp} for the factor profiles (top) and their summed contributions to total ion counts (bottom) for the final constrained seven-factor solution.

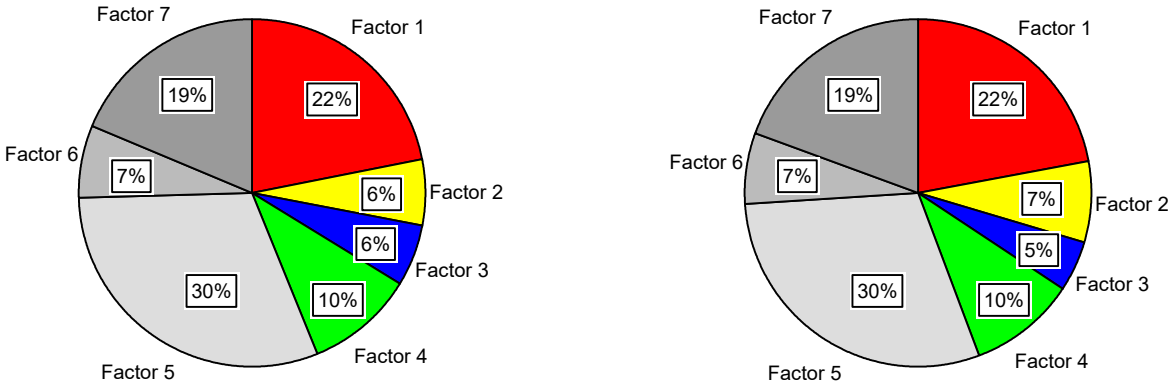

Figure S6. Average factor contributions to total ion counts (ncps) for the base (left) and constrained (right) seven-factor solutions.

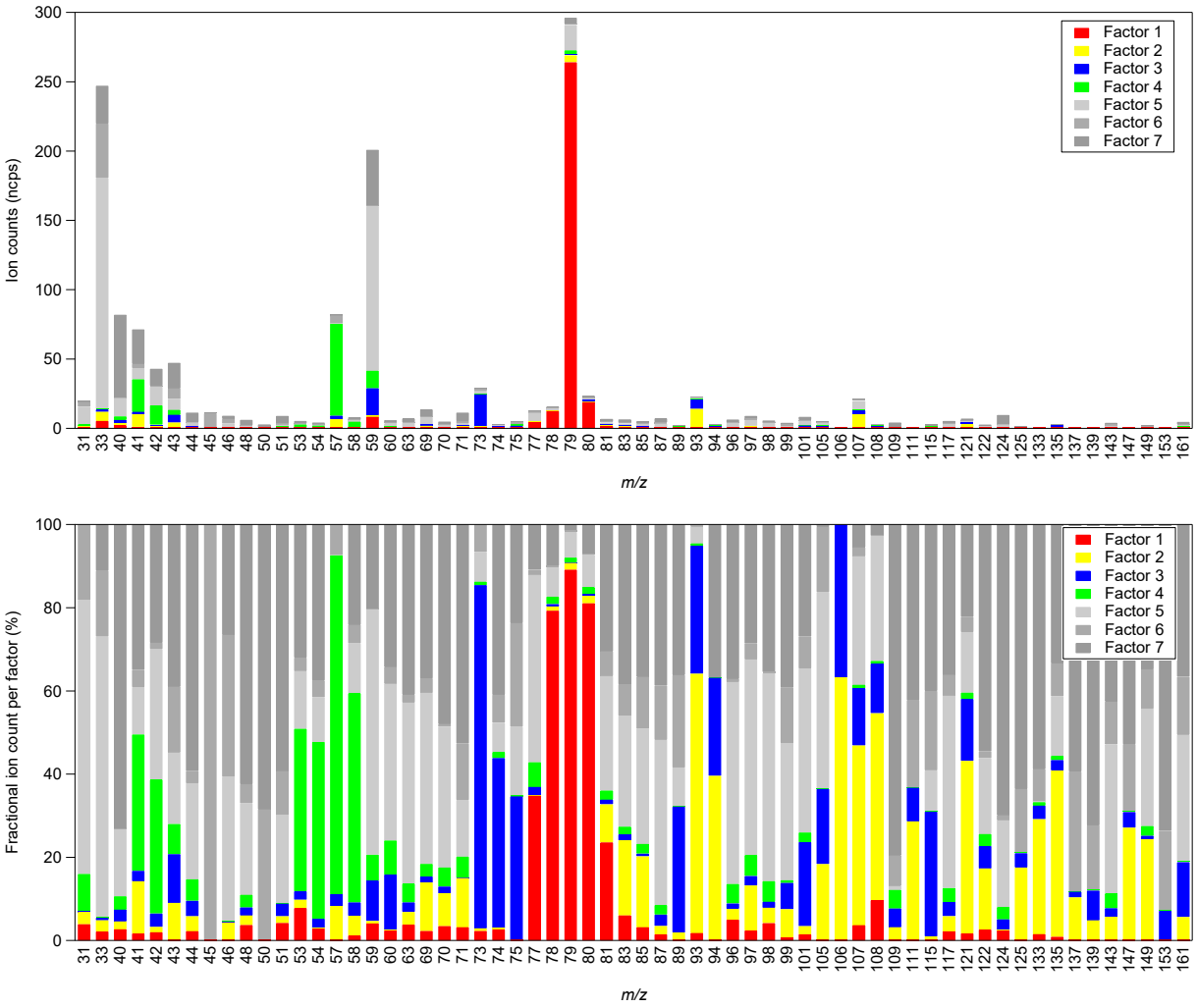

Figure S7. Factor contributions to total ion counts (ncps) for each *m*/*z* for the base seven-factor solution.

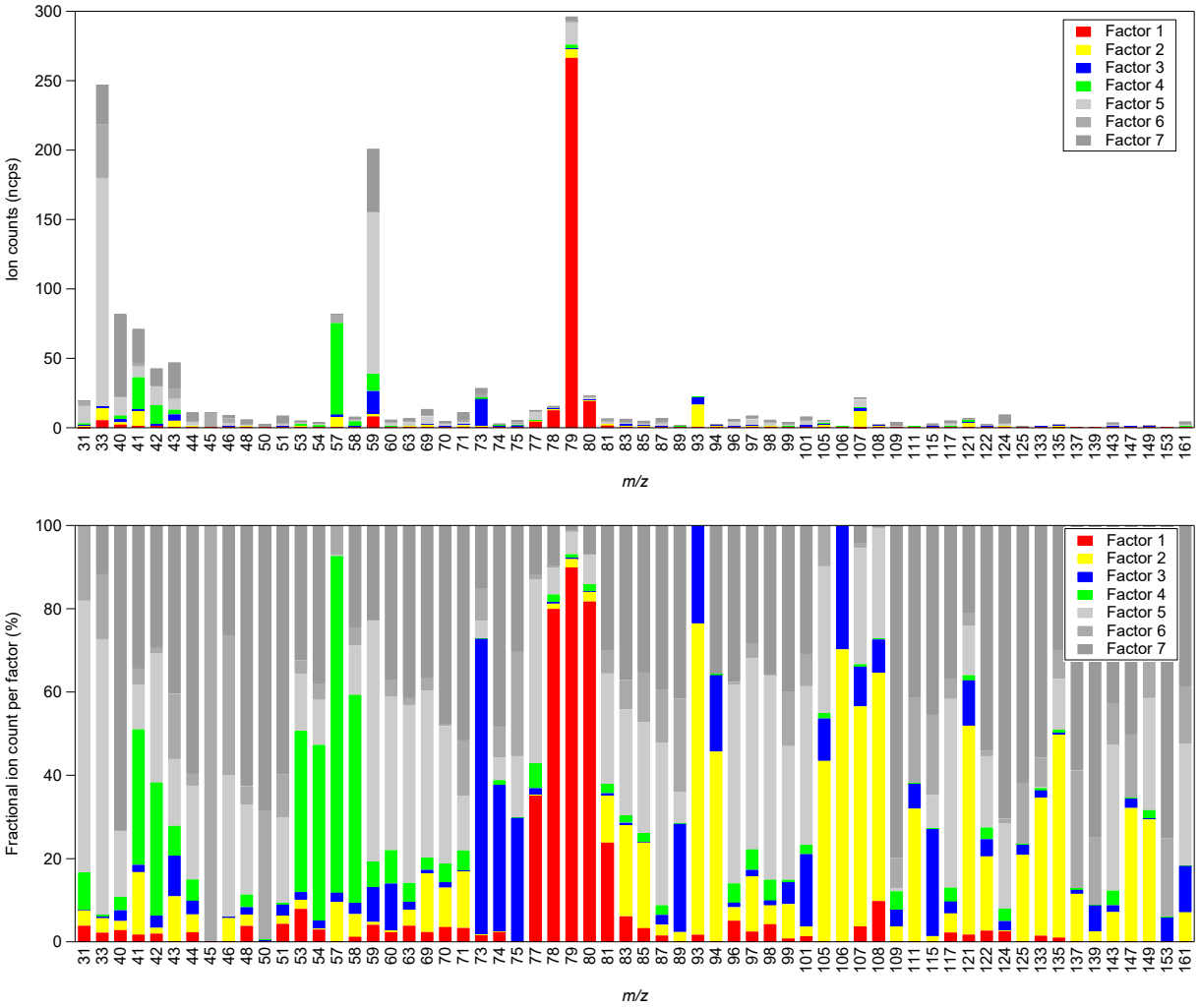

Figure S8. Factor contributions to total ion counts (ncps) for each *m*/*z* for the final constrained seven-factor solution.

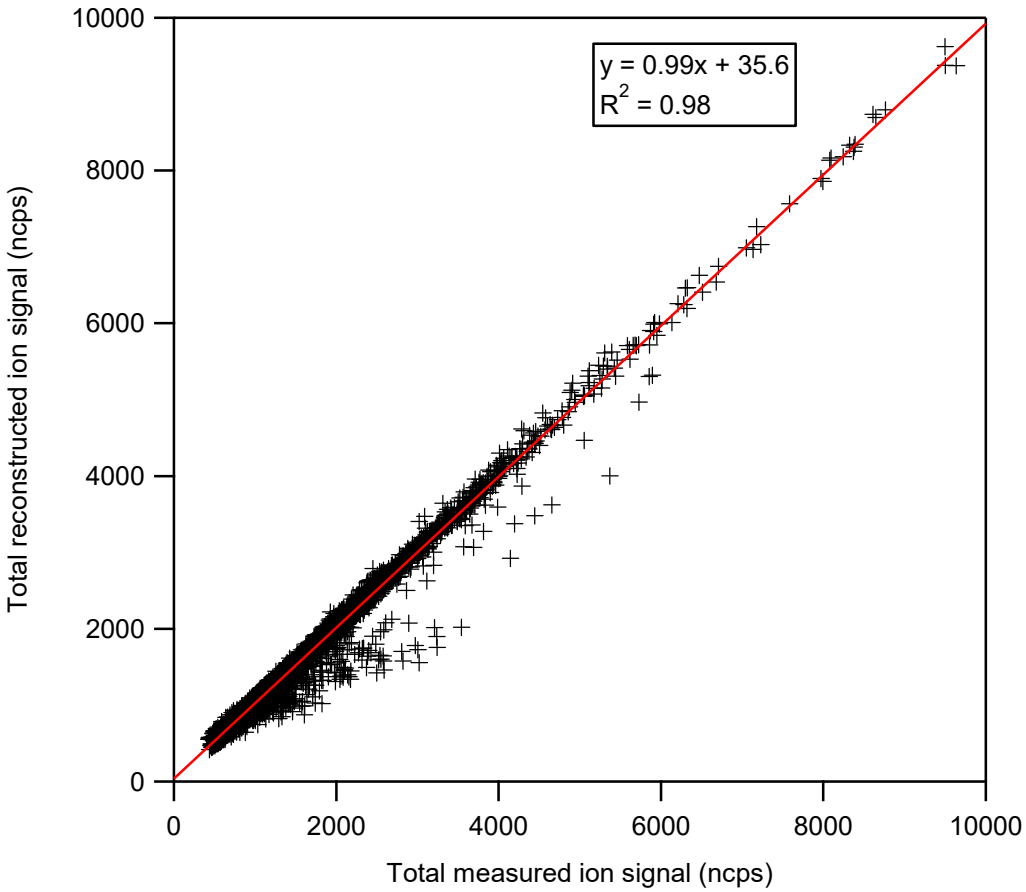

Figure S9. Relationship between reconstructed total ion signal and measured total ion signal for the final constrained seven-factor solution.

Regional/Background factors:

As shown below (Figure S10), the mass spectral profiles for the three factors associated with regional/background sources are characterized by signals for oxygenated VOCs. All three factors have significant contributions at *m*/*z* 33, attributable predominantly to ambient methanol ($CH_3OH{\cdot}H^+$). Factor 5 and Factor 6 differ from each other in that the former is characterized by a relatively dominant signal for acetone at *m*/*z* 59 ($C_3H_6O{\cdot}H^+$), while the latter is instead characterized by a signal for acetaldehyde at *m*/*z* 45 ($C_2H_4O{\cdot}H^+$). Factor 5 has a relatively stable persistent contribution on all five measurement days as shown in Figure S11, while Factor 6 exhibited the highest contributions on Day 2 (June 17, 2020) in the early morning. Meteorological conditions were calm the night before and into the morning of June 17, suggesting that Factor 6 is likely at least partly related to oxidation of local primary emissions in the area. Factor 7, in contrast, contains contributions from acetone and methanol, but also features high signals in the range *m*/*z* 40-43, especially at *m*/*z* 40. Upon examination of the raw mass spectra, the signal at m/z 40 was at least partially attributable to the large shoulder from the water cluster ($H_2O{\cdot}H_3O^+$) at *m*/*z* 37. The factor contribution for Factor 7 is also temporally correlated with ambient relative humidity, as shown in Figure S12. Higher contributions for this factor are observed on those days with higher relative humidity. This relationship suggests that the response of the instrument for *m*/*z* 40 is affected to some extent by ambient humidity, likely through enhanced formation of water clusters under humid conditions. None of the three background/regional factors were found to be associated with primary local emission sources in the study area.

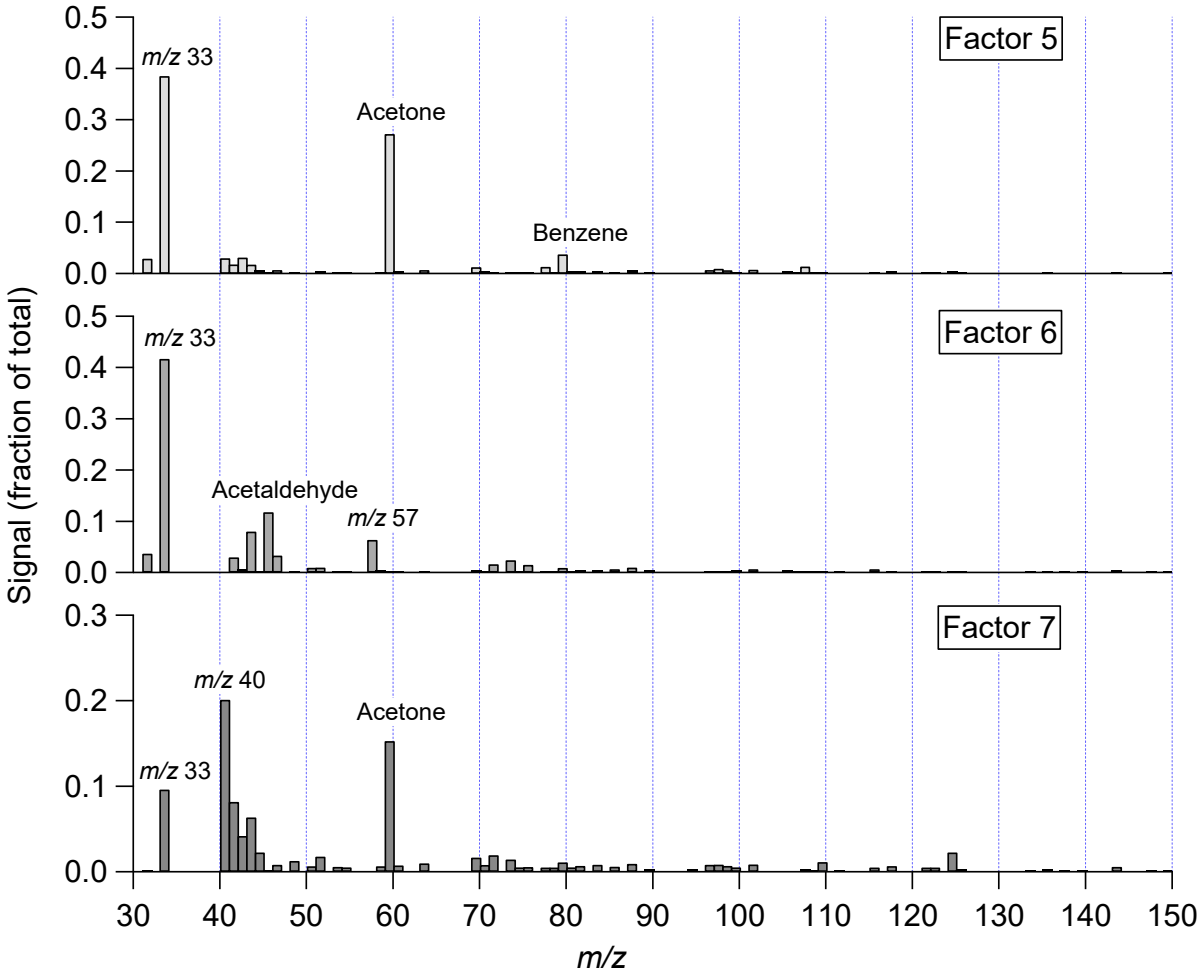

Figure S10. Mass spectral profiles for the three background factors.

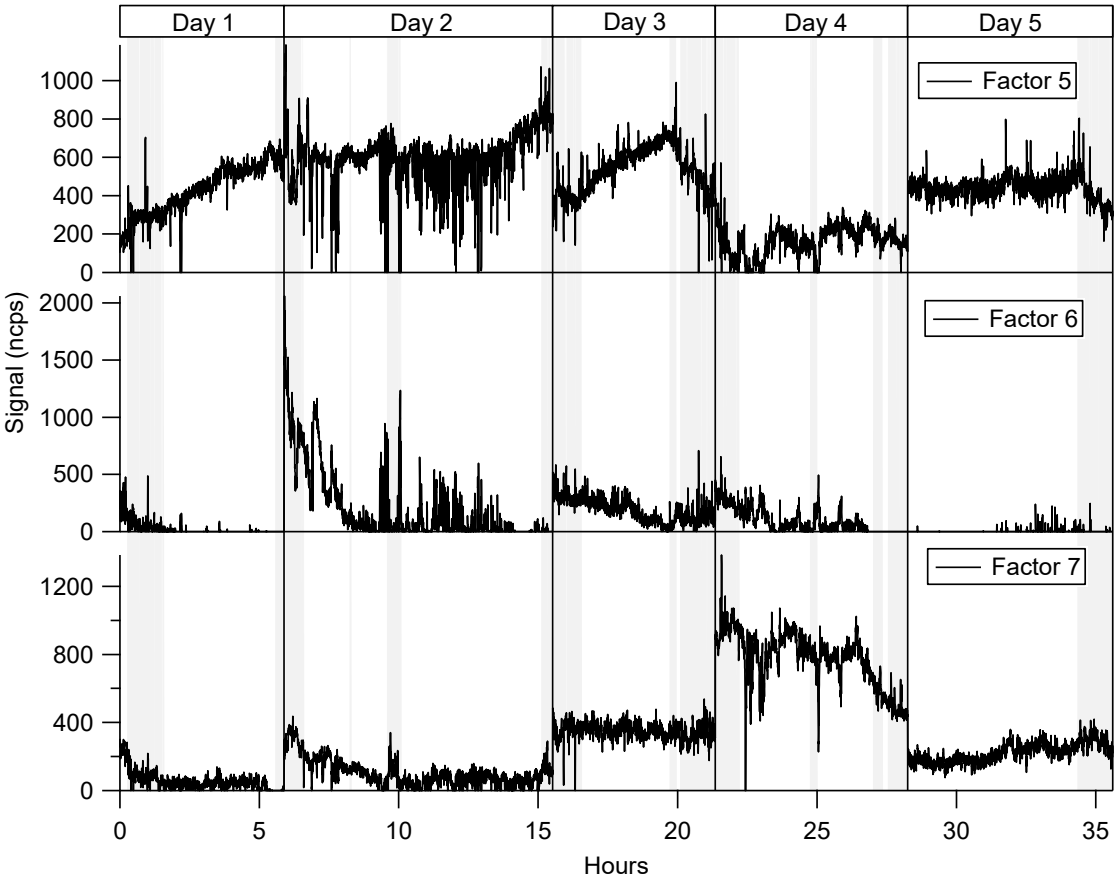

Figure S11. Temporality of factor contributions for the three background factors. Mobile monitoring periods are highlighted in grey and stationary monitoring periods are indicated by a white background.

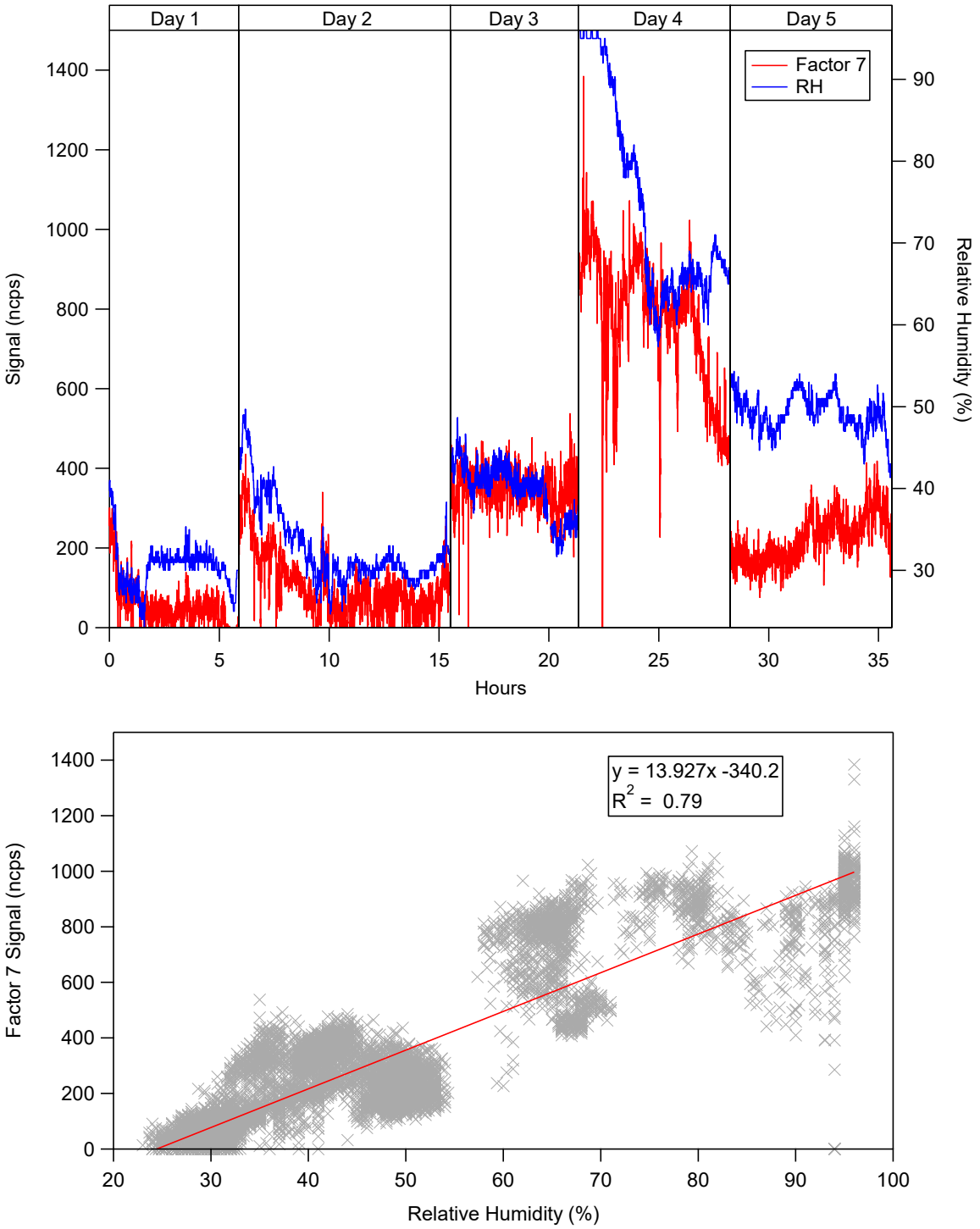

Figure S12. Temporality of the factor contribution for Factor 7 and ambient relative humidity (top) and linear regression of the factor contribution for Factor 7 and ambient relative humidity (bottom).

Stationary monitoring details:

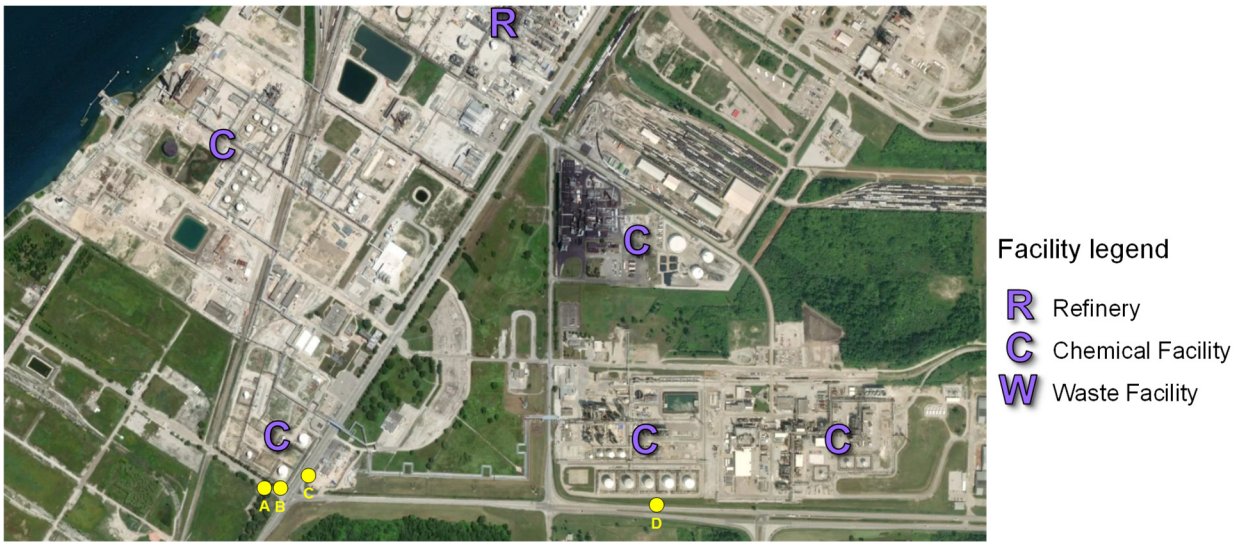

Figure S13. Stationary monitoring locations used on Days 1, 2 and 5.

Table S5. Stationary monitoring details for Days 1, 2 and 5.

Day	Date	Site	Start Time	End Time	Wind direction
1	16 June 2022	D	15:30	19:30	E/NE
2	17 June 2022	A	10:11	12:33	E/N
2	17 June 2022	B	14:49	19:19	N
5	24 June 2022	C	11:06	17:06	W

Figure S14. Stationary monitoring locations used on Days 3 and 4.

Table S6. Stationary monitoring details for Days 3 and 4.

Day	Date	Site	Start Time	End Time	Wind direction
3	18 June 2022	E	10:36	13:36	E/NE
4	23 June 2022	F	12:38	15:08	W
4	23 June 2022	G	15:25	17:25	SW

Conditional Probability Function Analysis

The on-board wind direction data, in combination with the PTR-ToF-MS measurement data can be used to identify the direction in which major sources are located. Conditional probability function (CPF) analysis is a receptor modelling tool applied to identify the likely location of VOC (and other pollutant) sources. CPF involves combining VOC measurement data with concurrent wind data to provide directional information on point sources [3]. CPF is calculated as follows:

CPF = $m_{\Delta\theta}/n_{\Delta\theta}$

where $m_{\Delta\theta}$ is the number of times wind was from a given direction and $n_{\Delta\theta}$ is the number of times that the specified threshold value for the VOC of interest (the 75th percentile), was exceeded while wind was from that direction. Five second resolution PTR-ToF-MS and 15° wind direction resolution data were used for the calculations. Figure S15 shows CPF results for benzene and butene data collected at Site A on Day 2. The highest benzene signals were observed when wind was from the direction of a nearby benzene storage tank, located at the south end of the southwesternmost chemical facility. In contrast, the highest butene levels were observed when wind was from the north/northwest, the direction of a rubber production facility which reports emissions of butene to air [4].

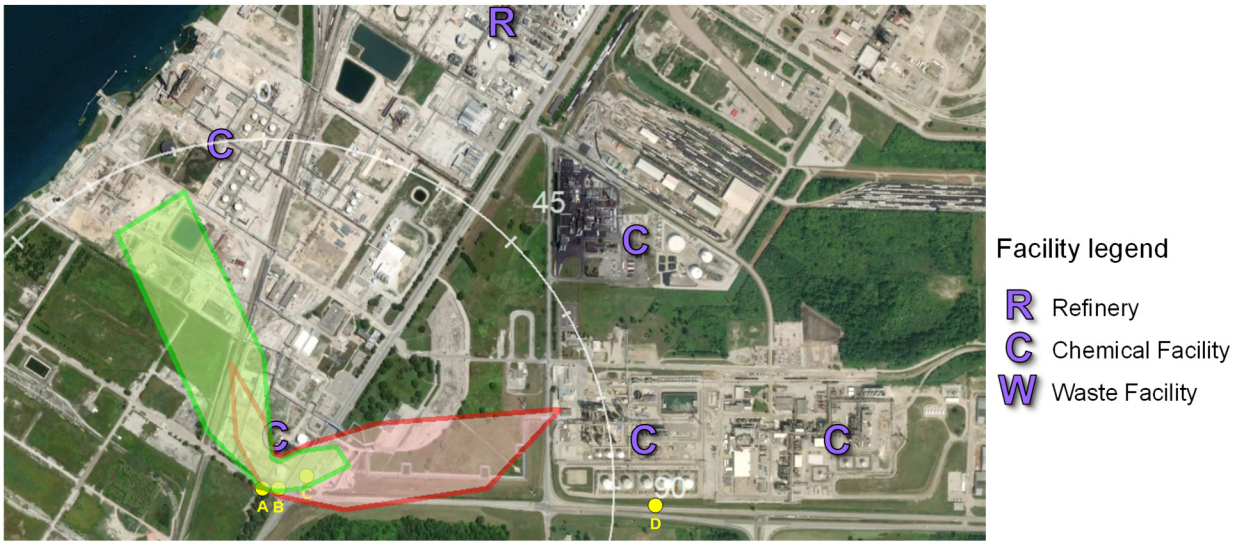

Figure S15. CPF plot illustrating the dependence of the highest signals (>75th percentile) measured for butene (green) and benzene (red) upon wind direction while stationary at Site A on Day 2.

Source apportionment results for individual species:

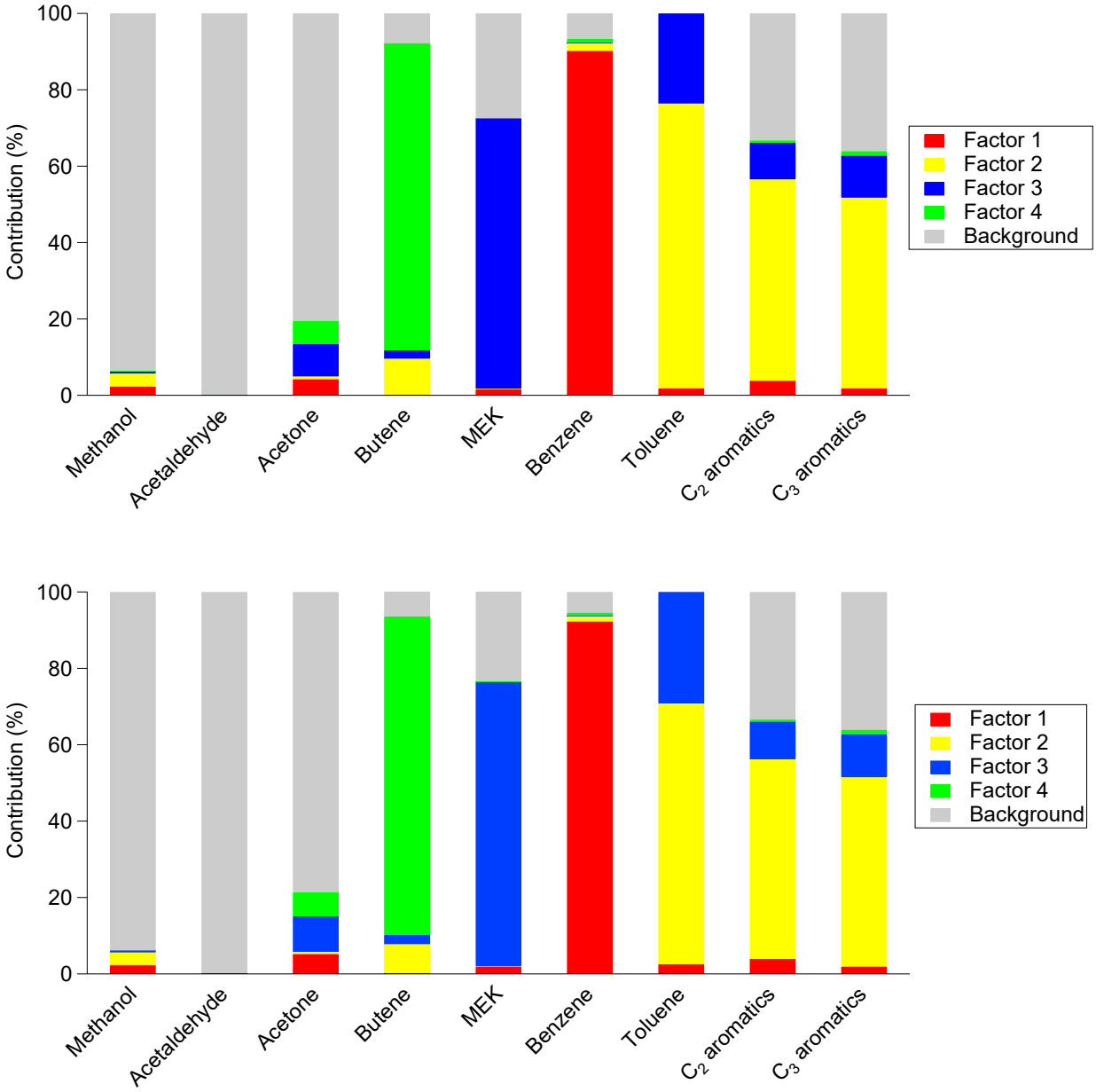

Figure S16. Apportionment of selected VOCs to the four local factors and the combined background factors for the entire study period (stationary and mobile) (top) and for stationary periods only (bottom).

Table S7. Apportionment of selected VOCs to the four local factors and the combined background factors for the entire study period (stationary and mobile).

	Factor 1	Factor 2	Factor 3	Factor 4	Background

Methanol	2.2	3.5	0.4	0.0	93.9
Acetaldehyde	0.0	0.0	0.0	0.0	100.0
Acetone	4.2	0.7	8.5	6.1	80.5
Butene	0.0	9.5	2.2	80.4	7.9
MEK	1.6	0.0	70.9	0.2	27.3
Benzene	90.1	2.0	0.0	1.1	6.7
Toluene	1.8	74.6	23.6	0.0	0.0
C_2 aromatics	3.8	52.7	9.6	0.6	33.3
C_3 aromatics	1.8	49.9	10.9	1.2	36.1

Table S8. Apportionment of selected VOCs to the four local factors and the combined background factors for stationary periods only.

	Factor 1	Factor 2	Factor 3	Factor 4	Background
Methanol	2.2	3.4	0.4	0.0	93.9
Acetaldehyde	0.0	0.0	0.0	0.0	100.0
Acetone	5.2	0.6	9.3	6.3	78.6
Butene	0.0	7.7	2.4	83.4	6.5
MEK	1.9	0.0	74.5	0.2	23.4
Benzene	92.2	1.4	0.0	0.9	5.5
Toluene	2.5	68.3	29.2	0.0	0.0
C_2 aromatics	3.9	52.2	9.8	0.6	33.4
C_3 aromatics	1.9	49.6	11.1	1.3	36.1

References:

1. Norris, G.; Duvall, R.; Brown, S.; Bai, S. *EPA Positive Matrix Factorization (PMF) 5.0 Fundamentals and User Guide 2014*; U.S. Environmental Protection Agency: Washington, DC, USA, 2014.
2. Sofowote, U.M.; Su, Y.; Dabek-Zlotorzynska, E.; Rastogi, A.K.; Brook, J.; Hopke, P.K. Constraining the Factor Analytical Solutions Obtained from Multiple-Year Receptor Modeling of Ambient PM2.5 Data from Five Speciation Sites in Ontario, Canada. *Atmospheric Environment* **2015**, *108*, 151–157, doi:10.1016/j.atmosenv.2015.02.045.
3. Ashbaugh, L.L.; Malm, W.C.; Sadeh, W.Z. A Residence Time Probability Analysis of Sulfur Concentrations at Grand Canyon National Park. *Atmospheric Environment (1967)* **1985**, *19*, 1263–1270, doi:http://dx.doi.org/10.1016/0004-6981(85)90256-2.
4. ECCC Environment and Climate Change Canada National Pollutant Release Inventory. 2019. Available online: https://www.canada.ca/en/environment-climate-change/services/national-pollutant-release-inventory/tools-resources-data/access.html (accessed on 13 April 2021).